Brazing vs. diffusion welding of graded Fe based matrix composite and yttria stabilized zirconia

Marie-Noëlle Avettand Fenoël, Kaoutar Naji, Ph Pouligny

Brazing *vs.* diffusion welding of graded Fe based matrix composite and yttria stabilized zirconia.

M.-N. Avettand-Fènoël[a,*], K. Naji[a,b], Ph. Pouligny[b]

[a] Univ. Lille, CNRS, INRA, ENSCL, UMR 8207 - UMET - Unité Matériaux et Transformations, 59000 Lille, France
[b] SNCF Réseau, Direction Ingénierie et Projets, 93574 La Plaine Saint Denis, France

* Corresponding author – E-mail: marie-noelle.avettand-fenoel@univ-lille.fr
Tel: 33(0)320436927

Abstract

Two graded Fe based matrix composite (MMC) – yttria stabilized zirconia (YSZ) joints were developed by brazing with Ticusil™ braze and by diffusion welding. The brazed joint was formed by solidification. During reactive brazing, some few micrometers thick continuous TiO_2, $Fe_2Ti_3O_9$ and $FeTiO_3$ layers were developed at the interfaces of the braze with both YSZ and MMC. On MMC side, TiO_2 was formed by reduction of FeO, stemming from MMC, by Ti. The formation of $Fe_2Ti_3O_9$ and $FeTiO_3$ compounds on YSZ side resulted from the combination of Fe and Ti which diffused through the braze, and O provided by YSZ and dissolved in the braze. The diffusion joint was developed by solid state sintering and YSZ-YSZ, YSZ-FeO and YSZ-Fe discontinuous bonds were created at the MMC-YSZ interface. During 3 points static bending tests, the diffusion joint showed a greater bending resistance compared to the brazed one. Some ways of optimization were finally proposed.

Keywords

Brazing; diffusion welding; metal matrix composite; ceramic; microstructure; mechanical properties.

1. Introduction

The combination of performing functional and mechanical properties to meet specifications of industrial applications generally requires the assembly of dissimilar materials such as ceramics and alloys or metallic matrix composites (MMCs). However ceramics present both ionic and covalent bonds while MMCs essentially present metallic bonds. These materials further present distinct physico-chemical and mechanical properties, which makes their joining a challenge.

Various processes are used to join such distinct classes of materials, namely

(i) mechanical joining which does not lead to an atomic bonding between the materials, and

(ii) joining processes which proceed

a. either at the liquid state such as brazing, melting with eutectic liquid, squeeze casting, field assisted bonding, soldering **[1]**, electron beam welding, (partial) transient liquid phase bonding and anodic bonding/electrostatic bonding/field assisted bonding **[2,3]**. In this case, various issues for their joining must be underlined, such as (i) the wettability of the ceramic by the metal which governs the quality of the atomic bonding at the interface, (ii) the eventual formation of thick interfacial layers of brittle phases deleterious for joint mechanical resistance and (iii) the mismatch of coefficients of thermal

expansion **[3]** and of Young moduli **[4]** originating some thermal residual stresses upon cooling.

b. or at the solid state like friction welding **[1]**, friction stir welding **[5,6]**, diffusion welding **[7,8]**, microwave welding, ultrasounds welding **[2,3]**, cold spray **[9,10]**. The use of solid state joining processes, which overcomes the wetting topic, should limit the excessive growth of brittle compounds at joint interface and may be expected to limit the thermal residual stresses.

In the railway sector, railway tracks need insulated joints to be inserted in the rail. This application requires to develop materials presenting at once electrical insulation and high mechanical properties; a novel architectured design of joint between graded Fe based MMCs and a yttria stabilized zirconia (YSZ) thin layer has been proposed **[11]**. First tests enabled to develop the graded MMCs (presenting a graded microstructure with an increasing volume fraction of reinforcements along the material, conferring them an evolution of their mechanical and/or functional properties) as a first step **[12]**, and to join them to the YSZ layer as a second step. Two joining processes were considered, namely diffusion welding and brazing with an Ag-Cu based braze. As aforesaid, given the different natures of the atomic bonds in YSZ (covalent and ionic) and in the braze (metallic), the ceramic – metallic braze joining is ticklish. This is the reason why various means were developed in literature to improve the wettability of YSZ by the Ag-Cu based braze, such as

(i) the coating of YSZ with a metal **[~~2,3,4,20,21~~2,3,4,13,14]**,

(ii) the introduction of TiH_2 in the braze and the coating of zirconia with TiH_2 leading to TiH_2 decomposition during brazing entailing the formation of a Ti layer on zirconia substrate **[~~22,23~~15,16]**,

(iii) the insertion of an active metal in the braze such as Ti (with a content in-between 2 and 5% **[~~1,2,~~41,2,4,17]**). The active metal modifies the surface chemistry of the ceramics, diminishes its surface energy by forming an intermediate reaction layer and reduces the contact angle of the melted braze on YSZ **[~~2,18,21,24~~2,14,18,19]**.

It is the latter solution, that is the insertion of Ti active metal in the braze, which was chosen during the current study. A satisfactory braze must wet but should also be ductile and bond strongly **[~~20~~13]**. The Ag-Cu braze is a ductile solvent in which Ti has a very high activity coefficient, which is the relevant thermodynamic parameter that governs the interfacial reaction **[~~25~~20]**, so that there is no major reservoir of Ti from which too thick brittle reaction product layers may form.

The current paper aims to understand the formation mechanisms of the joints developed by diffusion welding and by brazing, and to compare their ~~microstructural architecture~~ microstructure and ~~their~~ mechanical properties. The pros and the cons of each process in connection with the performances of the joints will finally be discussed.

2. Experimental procedure

The base materials to assemble are 10 mm diametered and 1 mm thick sintered zirconia stabilized with 3 mol.% yttria (YSZ) layers supplied by Umicore® (table 1) and graded oxide dispersion strengthened (ODS) Fe based composites (diameter of 10 mm and average thickness of 7 mm). The latter material developed by high energy ball milling, compaction and sintering consists in a stacking of various composite subparts with incremental volume fractions (V_f) of YSZ particle reinforcements (V_f =0 – 0.05 – 0.1 – 0.2 – 0.3 – 0.4). The subpart that contains the greatest volume fraction of YSZ is the one to be joined to YSZ layer. For further information about the design, the development and the characterization of the graded metal matrix composite (MMC), the reader is encouraged to refer to a previous paper of the authors **[12]**.

Table 1: Chemical composition (mass. %).

Material	ZrO_2	Y_2O_3	Fe_2O_3	Na_2O	Ag	Cu	Ti	Al	Bi	Cd	P	Pb	Si
YSZ	94.8	5.2	<0.01	<0.01	-	-	-	-	-	-	-	-	-
Ticusil™	-	-	-	-	68.8	26.7	4.5	<0.001	<0.03	<0.01	<0.008	<0.025	<0.05

Two joining processes were tested to assemble the base materials: brazing and diffusion welding.

Concerning brazing, a 51 µm thick ribbon of Ticusil™ braze (table 1) provided by Johnson Matthey® was used as filler metal between the YSZ layer and the graded MMCs. The ~~braze~~ solidus temperature and the liquidus temperature~~s~~ of the braze ~~amount to~~are 778°C and 850°C respectively, according to the supplier.

In a first step, the YSZ wettability by the braze was analyzed with the sessile drop method **[~~16~~21]**. The wettability tests were performed under secondary vacuum with roughly or finely polished YSZ substrates surfaces. Two automatic and then reproducible polishing procedures of materials were indeed set up leading to rough and fine surfaces with suspensions containing particles with a size respectively greater and lower than 1 µm so as to investigate the effect of the substrate roughness on the wettability by the braze. The roughness and the Ra parameter (defined as the mean arithmetic roughness of the analyzed surface) of both the YSZ layers and the most charged composite subpart of graded MMC were characterized with a 3 D optical profiler WYKO NT1100®. The evolution of the aspect of the braze drop put on the substrate was recorded as a function of temperature and time with a charge coupled device (CCD) camera. The contact angle (wetting angle) between braze and substrate could thus be directly measured on the sideways images of the drop captured by the digital camera (such as those in figure 5) using the ImageJ™ image processing software.

In a second step, brazing was carried out in a home-made TZM (Mo based alloy with 0.5% Ti, 0.08% Zr and 0.03% C) device under a uniaxial pressure of 40 cN and secondary vacuum (2.6×10^{-7} atm). The brazing cycle is depicted in figure 1a. It was chosen according to literature recommendations **[~~13~~22]**. The 5 min holding time at 750°C enabled to homogenize the temperature along the materials stacking before reaching the brazing temperature of 900°C. The choice of performing no holding time at 900°C was made in order to avoid composite microstructure coarsening during brazing and the formation of too thick interfacial layers prohibitive for joint mechanical resistance. The low cooling rate of 5°C/min was used to limit the thermal residual stresses which may be generated at the joint interfaces because of the difference of thermal expansion coefficients (CTE) between the braze (18.5×10^{-6} $°C^{-1}$ **[~~14~~23]**), YSZ (9.6×10^{-6} $°C^{-1}$ over [20-400°C] range according to the supplier) and the Fe based graded composite (14.6×10^{-6} C^{-1} over [20-800°C] for Fe CTE [**~~15~~24**]).

With regard to diffusion welding, joining occurred simultaneously with graded ODS MMC sintering. Diffusion welding cycle, namely sintering cycle, is displayed in figure 1b. Sintering was performed in a free radial stresses matrix under a uniaxial pressure of 50 kPa and secondary vacuum (2.6×10^{-7} atm).

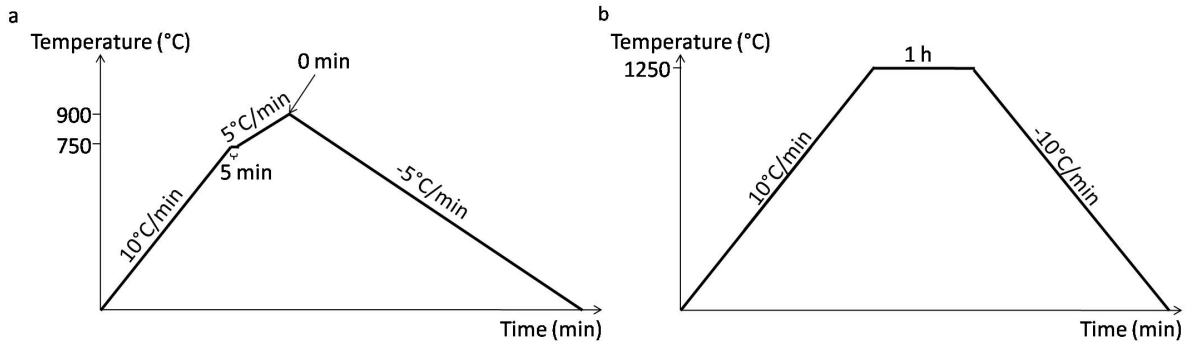

Figure 1: Brazing (a) and diffusion welding (b) cycles.

~~The roughness and the Ra parameter (defined as the mean arithmetic roughness of the analyzed surface) of both the YSZ layers and the most charged composite subpart of graded MMC were characterized with a 3-D optical profiler WYKO NT1100®. Two automatic and then reproducible polishing procedures of materials were set up leading to rough and fine surfaces with suspensions containing particles with a size respectively greater and lower than 1 µm so as to investigate the effect of the substrate roughness on the wettability by the braze. The YSZ wettability by the braze was analyzed with the sessile drop method [16]. The wettability tests were performed under secondary vacuum with roughly or finely polished YSZ substrates surfaces. The evolution of the aspect of the braze drop put on the substrate was recorded as a function of temperature and time with a charge coupled device (CCD) camera. The contact angle (wetting angle) between braze and substrate could thus be directly measured in the photographies.~~

Both joints were cut along the longitudinal direction and polished up to 1 µm. Their microstructure was then characterized by scanning electron microscopy (SEM) with a JSM 7800F, JEOL® microscope equipped with secondary electrons (SE) or back scattering electrons (BSE) mode and X-ray energy dispersive spectroscopy (EDX).
The phases crystallography was identified by X-ray diffractometry performed in a Philips X'Pert Pro® equipment using a Bragg-Brentano configuration and a Co anticathode with a wavelength of 1.78901 Å.

Finally, some 3 points static bending tests were carried out according to NF EN ISO 14125 standard **[~~17~~25]** on the 10 mm diametered and 15 mm thick joints (design of the brazed joint: graded MMC-braze-YSZ-braze-graded MMC and design of the diffusion joint: graded MMC-YSZ-graded MMC; for both joints, the greatest reinforcements volume fraction of the graded MMC is close to the YSZ layer (central part) of the joints). During bending tests, the upper mechanical support was a 5 mm diametered cylinder whose speed was 1 mm/min. It has been applied on the YSZ central layer of the joints. The 2 lower static supports were fixed at a distance of 3.25 mm from the centre of the joints. The load applied on the upper mechanical support was in-between 100 N and 20 kN. The fracture surfaces of the joints after bending tests were finally characterized.

3. Results

3.1. Base materials

3 mol.% yttria stabilized zirconia sintered commercial sample is characterized by a mean grain size smaller than 0.5 µm. In order to investigate the effect of ceramic roughness on its wettability by the braze, two tetragonal YSZ commercial sintered samples were

polished with two different procedures qualified of (i) either rough polishing leading to a mean roughness of 257 nm (figure 2a and b), or (ii) fine polishing entailing a mean roughness of 63 nm (figure 2c and d).

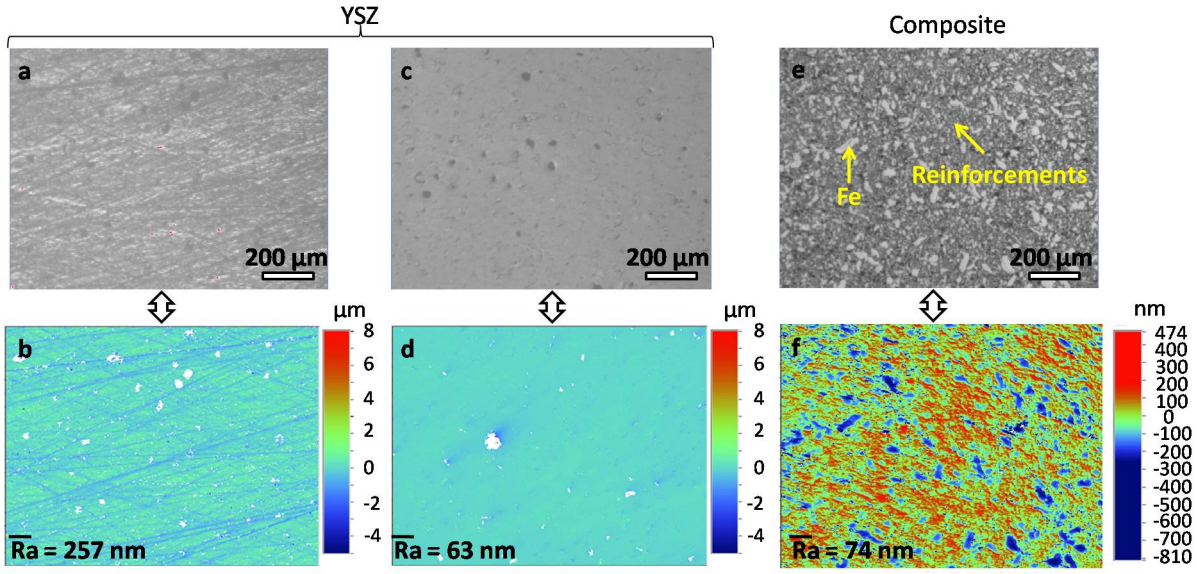

Figure 2: Surfaces of YSZ after rough (a) and fine (c) polishing (light microscopy) and their corresponding roughness maps (b and d, respectively). Surface of Fe-40vol.% YSZ composite after fine polishing (light microscopy) (e) and its corresponding roughness map (f). The color scales indicate the roughness level.

The graded Fe based composite is polyphase and is constituted of Fe grains (light grey colored) with an interconnected network of monoclinic zirconia and tetragonal yttria stabilized zirconia (white colored), and of wüstite (FeO) (dark grey colored) (figure 3) **[12]**. The FeO content was shown to not evolve in the various composite subparts of the MMC **[12]**. For further information about the graded composite, the reader may refer to a previous paper of the authors **[12]**. The surface state of the composite seems to be more uneven than that of YSZ (the color scales of figures 2d and f are however different) and its mean roughness amounts to 74 nm (figure 2e and f).

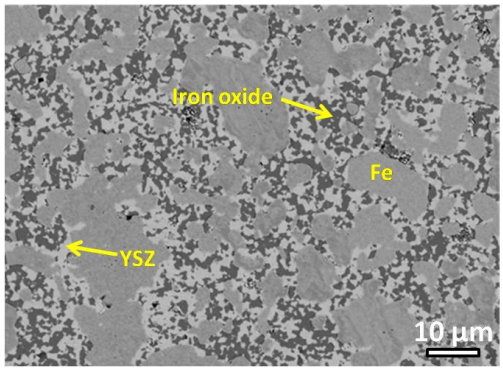

Figure 3: Details of the polished microstructure of the Fe-40 vol.% YSZ subpart of the graded metallic matrix composite (BSE/SEM).

The Ticusil^{TM} interlayer presents an average thickness of 54 µm. It is a sandwich shaped film constituted of two layers of Ag-Cu eutectic alloy inserting a Ti layer with an uneven thickness (figure 4); according to EDX analyses, it contains 68% Ag, 27% Cu, 5% Ti (mass%) (54.3%Ag-36.6%Cu-9.1%Ti (at.%)), which is consistent with supplier's data (table 1). It is worth noting that the Ti content is sufficient to render the braze active, according to

literature data **[1,2,4]**. The latter Ti content in the braze is also known to improve the 4 points bending strength of YSZ-YSZ brazed joints **[18]**.

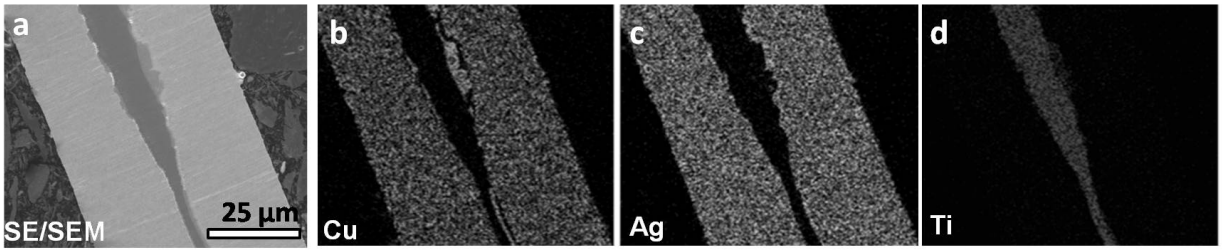

Figure 4: Transverse cross section of Ticusil^{TM} braze film (a) (SE/SEM) and associated Cu Kα (b), Ag Lα (c) and Ti Kα (d) X-ray maps (EDX).

3.2. Joints microstructure

3.2.1. Brazed joint

3.2.1.1. Contact angle and wetting kinetics.

Figure 5 displays an example of the evolution of YSZ wettability by Ticusil^{TM} braze with temperature according to the sessile drop method. It shows the progressive spreading of the braze on the substrate. At its solidus temperature close to 780°C, the braze begins spreading on the substrate. At 900°C, the drop is shiny (figure 5), which means that it is mostly liquid; its angle contact is close to 57.5°. At 950°C, the drop of Ticusil^{TM} spreads more on the YSZ surface and the contact angle reaches 54°.

Figure 6a depicts the effect of the surface roughness of YSZ and of the brazing temperature on YSZ wetting by Ticusil^{TM} braze. It is worth noting that the lower the YSZ surface roughness, the smaller the wetting angle is. In addition, whatever the roughness, the wetting angle is reduced with an increase of the brazing temperature. In order to avoid the coarsening of the microstructure of the graded composite, it was decided to braze at 900°C (figure 1a) the composite and YSZ, both finely polished. Figure 6b shows a reduction of the wetting angle of the braze on the YSZ finely polished up to 20 minutes spent at 900°C. From this time, the wetting angle remains constant. However, in order to avoid (i) a too marked growth of the braze – YSZ and braze – graded composite interfacial layers and (ii) a coarsening of the graded composite microstructure, no soaking at the brazing temperature of 900°C was considered (see figure 1a).

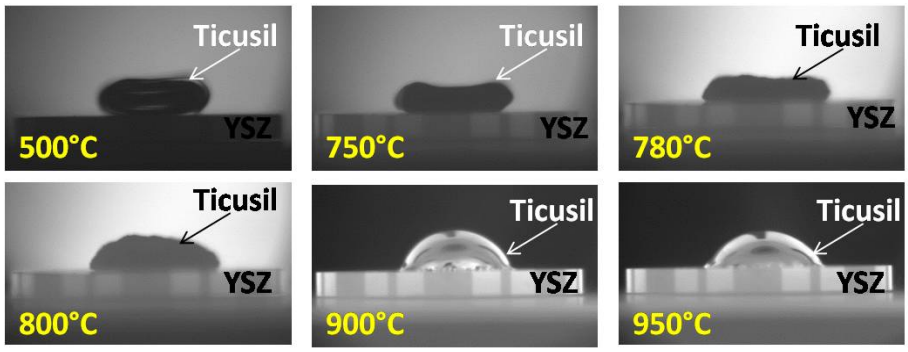

Figure 5: Effect of temperature on ~~YSZ (finely polished) wettability by~~Ticusil^{TM} braze spreading on YSZ (finely polished) (sessile drop method) [the thickness of YSZ sample is about 1.5 mm].

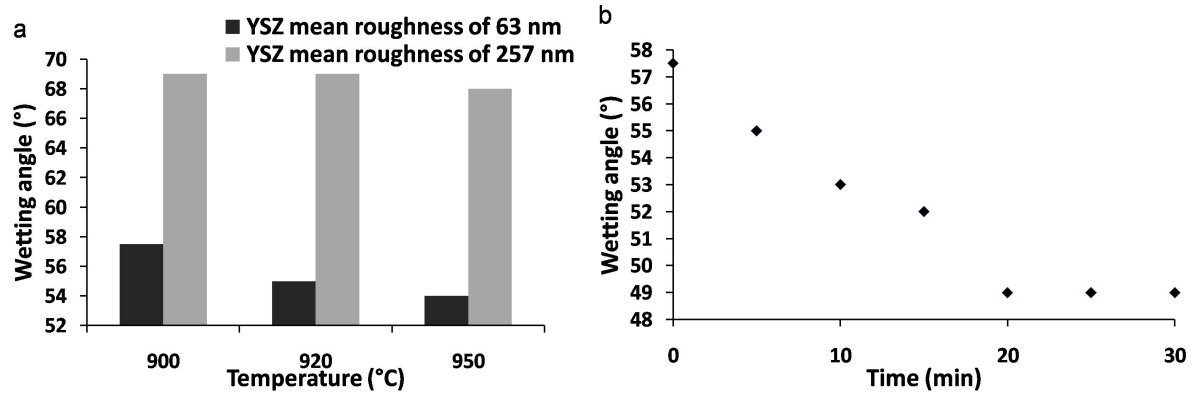

Figure 6: a) Effect of different roughness values and of temperature on contact angle between Ticusil™ braze and YSZ substrate. A constant mass of 0.14 g of braze was used for the experiments. b) Effect of time at a brazing temperature of 900°C on wetting angle of Ticusil™ braze (mass of 0.158 g) on YSZ surface presenting a mean roughness of 63 nm. ~~The contact angle values were measured on the sideways images of the drop captured by the digital camera (such as those in figure 5) using the ImageJ™ image processing software.~~

3.2.1.2. Microstructure of the graded composite – YSZ brazed joint at 900°C.

Compared to the 54 µm primitive braze film thickness (figure 4), the interfacial zone thickness of the brazed joint amounts to only 15 µm at most (figures 7 and 8) because of the pressure applied on the stacked materials and of the solid-liquid transition of the braze during heating step.

The transverse cross section of the brazed joint is displayed in figure 7. On the composite side and from the composite-braze interface, it is worth noting a depletion in iron oxides over a thickness of about 12 µm (figure 7).

The braze – YSZ interface is straight while the braze – composite interface is wavy. The first one is about 1 µm thick while the second one is at most 10 µm thick (figures 7 and 8).

The central part [layer 3] of the interfacial zone is composed of the eutectic constituent made of 2 phases, namely a predominant Ag based phase enriched in Fe, Cu and O (point 6, figure 8) and a Ti based one enriched in Fe, Cu and O (point 5, figure 8).

From the composite, the composite-braze interface is successively made of

(i) a Ti and O bearing layer [layer 1] (point 3, figure 8) with Fe and zirconia rich islands (point 2, figure 8), stemming from the composite and

(ii) a Cu and O bearing Ti and Fe based layer [layer 2] with an atomic ratio Fe/Ti equal to 0.5 (point 4, figure 8). This layer is crossed by the eutectic constituent (see yellow arrows in figure 8c and d).

The braze-YSZ interface is constituted of a Cu and O bearing Fe and Ti based phase [layer 4] with an atomic ratio Fe/Ti equal to 0.5 (point 7, figure 8) with a similar composition as point 4, figure 8 in layer 2.

These observations indicate that Ti diffused from the centre of the primitive braze (figure 4) towards the composite and penetrates into it over a distance up to 10 µm (figure 8a and f). Fe stemming from the composite is detected up to the YSZ-braze interface in Ti rich phases and in the eutectic constituent. The Fe diffusion distance is about 10 µm (figure 8a and b).

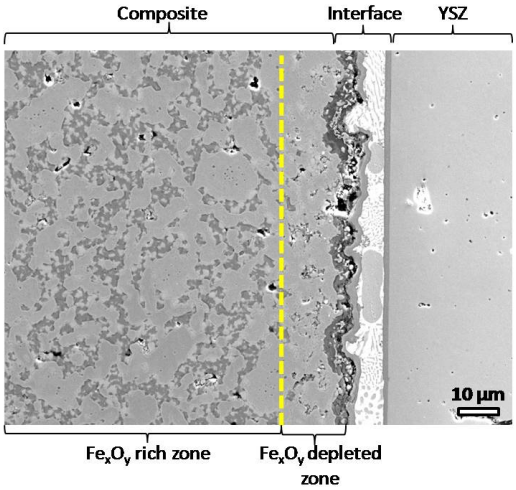

Figure 7: Global view of the transverse cross section of the interface of the brazed [Fe - 40 vol.% YSZ composite / YSZ] joint (BSE/SEM).

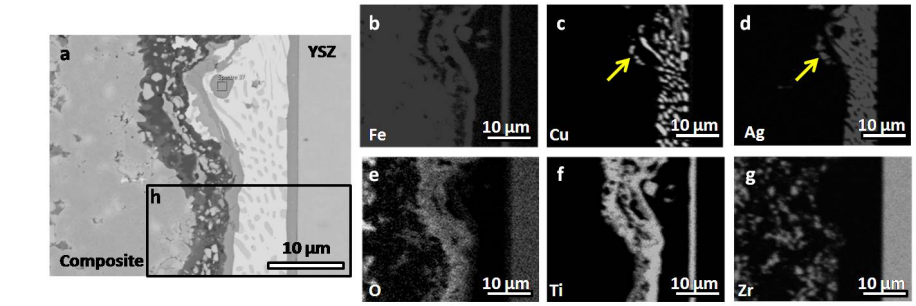

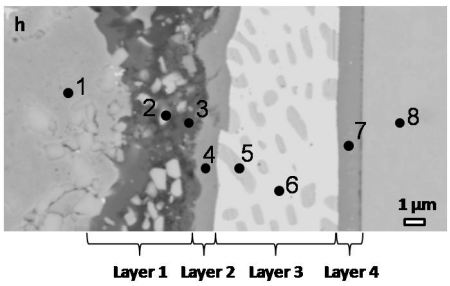

at.%	Fe	Ti	Cu	Ag	Zr	Y	O
1	100	0	0	0	0	0	no
2	9.6	3.1	0	0	77.9	9.3	+++
3	8	88	0	0	4	0	+++
4	31	59	10	0	0	0	++
5	8.3	87.5	4.2	0	0	0	+++
6	2	0	6	91	0	0	++
7	29	59	11	1	0	0	++
8	0	0	0	0	97	3	+++

Figure 8: Transverse cross section of the interface of the brazed [Fe - 40 vol.% YSZ composite / YSZ] joint (BSE/SEM) (a) and Fe Kα (b), Cu Lα (c), Ag Lα (d), O Kα (e), Ti Kα (f) and Zr Lα (g) X-ray maps (EDX/SEM). Magnified zone of micrograph a (h) and atomic compositions of the various phases reported in the table (the calculations are made without taking into account O content) (EDX/SEM).

3.2.2. Diffusion weld

Figure 9 depicts the MMC – YSZ interface features. Along the straight interface which is free of porosities, some punctual areas of sintering between YSZ sample and YSZ stemming from the composite are observed, which leads to discontinuous YSZ bonds between both parts of the diffusion joint. Some Fe-YSZ and FeO-YSZ bonds were also formed during solid state sintering at the interface, in the same way that the microstructure was formed in the graded composite from powder particles **[~~13~~12]**.

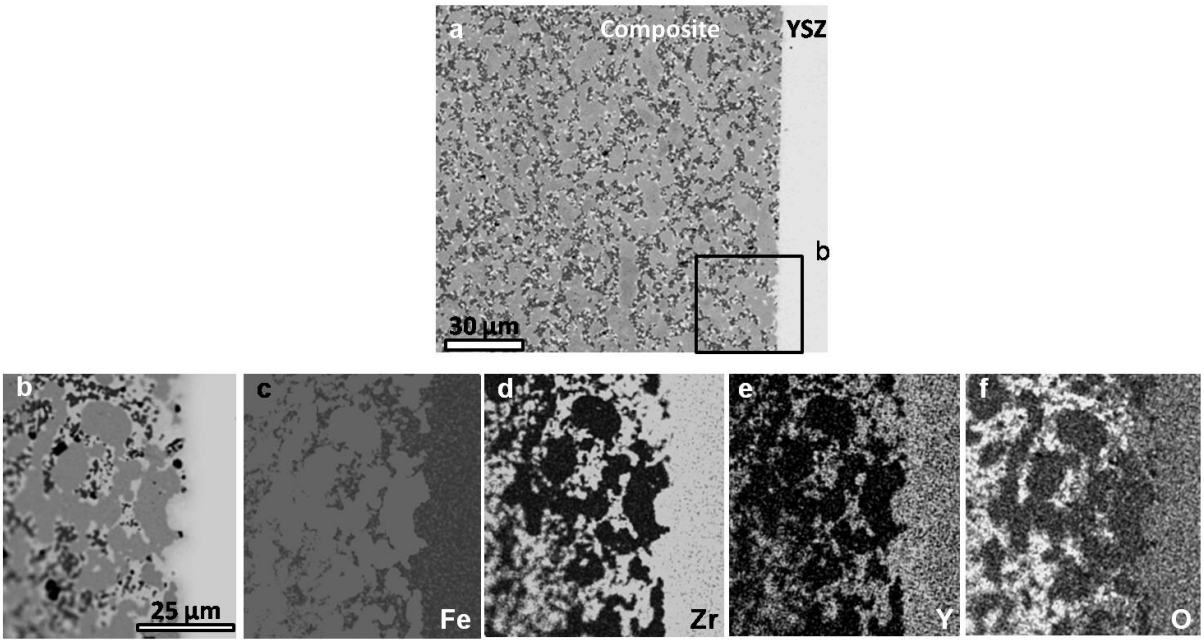

Figure 9: a) Global view of the transverse cross section of the [Fe - 40 vol.% YSZ composite / YSZ] diffusion joint interface and b) magnification of the black encircled area in figure (a) (BSE/SEM) with Fe Kα (c), Zr Lα (d), Y Lα (e) and O Kα (f) X-ray maps (EDX/SEM).

3.3. Joints mechanical properties

The global aspects of the laboratory scale joints are displayed in figures 10 a and b. According to the 3 points bending tests, the diffusion joint is twice more performing than the brazed joint in terms of maximum force and deflection. It is also 4 times tougher with regard to the fracture energy, despite its very low value (figure 10c).

Figure 11 depicts pretty smooth fracture surfaces on both MMC and YSZ sides of the brazed joint. XRD analyses prove that the brazed joint fracture surfaces are enriched in $Ti_3Fe_2O_9$, TiO_2 (rutile), $TiFeO_3$ and traces of Ag, Cu, Fe and YSZ (figure 12). The chemical composition of the first two compounds are consistent with EDX analyses on transverse cross section of the brazed joint (see composition of points 4 and 7, figure 8 with a Fe/Ti ratio of 0.5 close to that of 0.66 for $Ti_3Fe_2O_9$, and composition of point 3, figure 8 very likely consistent with TiO_2 phase). The whole results (with EDX analyses of the fractured surfaces (not shown here)) prove that the brazed joint rather fractured in layer 1 and maybe even also in layer 2 at the MMC-braze interface.

Concerning the diffusion joint, its fracture surfaces on MMC and YSZ sides displayed in figure 13 are also rather smooth. The EDX maps (figure 14) suggest that the fracture occurred at the MMC – YSZ interface.

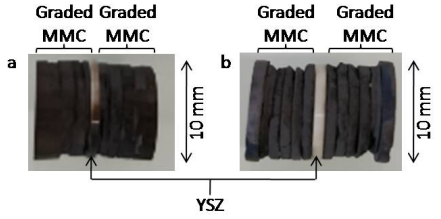

c

Joint	Maximum force (N)	Largest deflexion (mm)	Fracture energy (mJ)
Brazed	217	0.05	5.7
Diffusion	400	0.1	20.8

Figure 10: Brazed (a) and diffusion (b) joint features. Maximum force, largest deflection and fracture energy of both joints during 3 points bending tests (c).

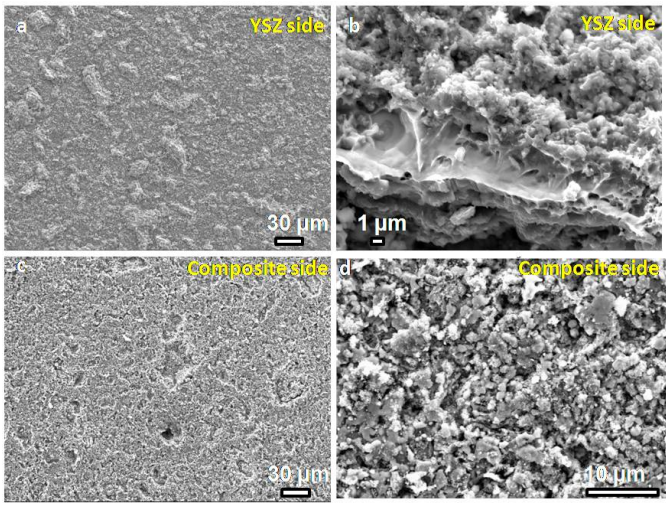

Figure 11: Fracture patterns of brazed joint after 3 points bending tests (SE/SEM).

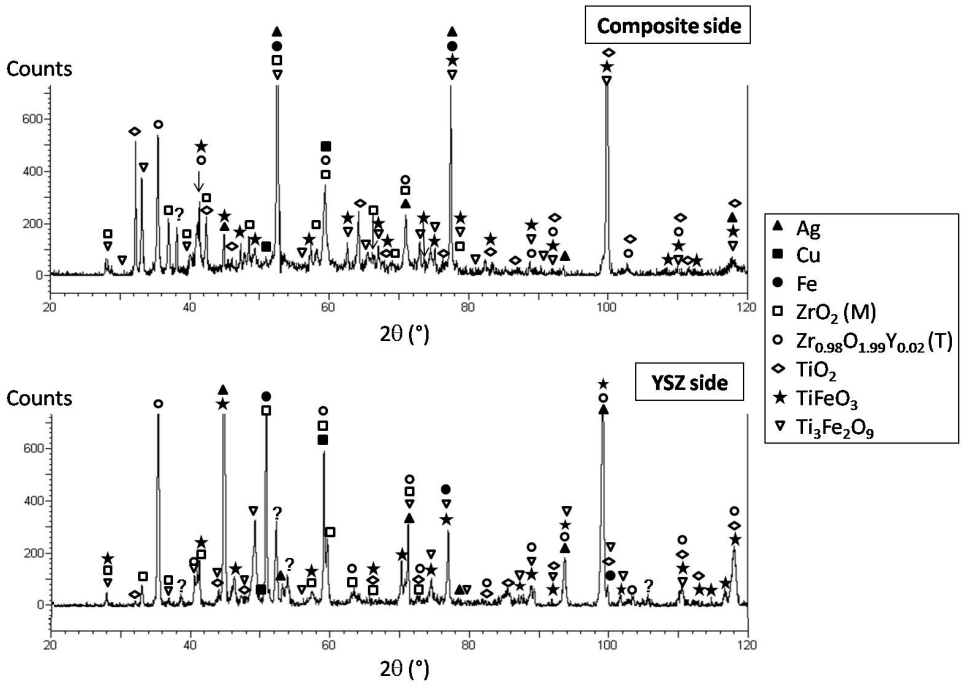

Figure 12: Magnified X-ray diffraction patterns of fracture surfaces of the brazed joint on composite (a) and YSZ (b) sides. M and T are the respective abbreviations of monoclinic and tetragonal crystal lattices.

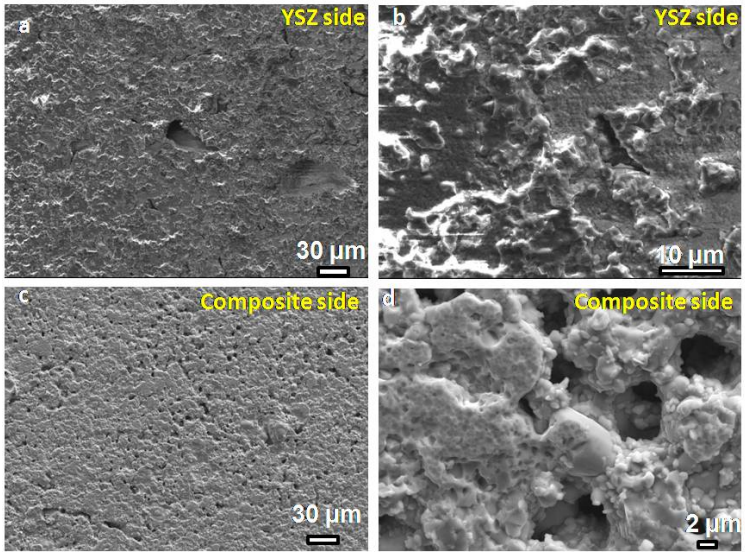

Figure 13: Fracture patterns of diffusion joint after 3 points bending tests (SE/SEM).

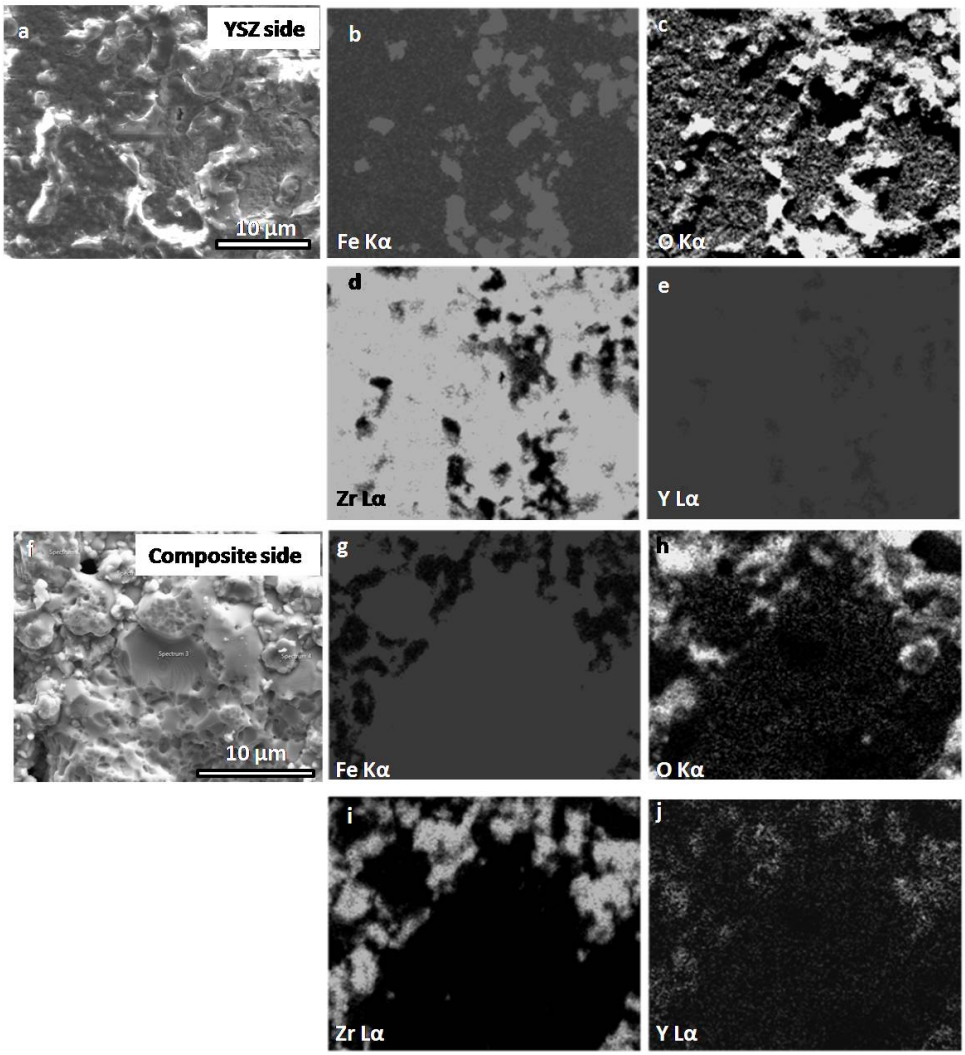

Figure 14: Fracture patterns of diffusion joint after 3 points bending tests: YSZ side micrograph (SE/SEM) (a) and Fe Kα (b), O Kα (c), Zr Lα (d) and Y Lα (e) X-ray maps; composite side micrograph (SE/SEM) (f) and Fe Kα (g), O Kα (h), Zr Lα (i) and Y Lα (j) X-ray maps (EDX/SEM).

4. Discussion

4.1. Brazing

4.1.1. Effect of Ticusil™ - YSZ brazing conditions on wettability, braze spreading kinetics and work of adhesion

4.1.1.1. Wettability

Four fundamental principles are required for suitable brazing **[~~13,19,20~~13,22,26]**, namely

(i) the wetting of the substrate by the braze,

(ii) the suitable capillarity of the braze (in the case of vertical configuration which is not the case in the configuration used for sessile drop method (figure 5)), the wettability and the capillarity being linked to the braze viscosity, which can evolve with brazing time and temperature in case of dissolution of chemical elements from the base material into the braze, and

(iii) the diffusion of braze elements in or towards the base material and the dissolution of the base material or diffusion of its elements in the braze leading to interfacial reactions.

~~As aforesaid, given the different natures of the atomic bonds in YSZ (covalent and ionic) and in the braze (metallic), the ceramic – metallic braze joining is ticklish. This is the reason why various means were developed to improve the wettability of YSZ by the Ag-Cu based braze, such as~~

~~(iv) the coating of YSZ with a metal **[2,3,4,20,21]**,~~

~~(v) the introduction of TiH_2 in the braze and the coating of zirconia with TiH_2 leading to TiH_2 decomposition during brazing entailing the formation of a Ti layer on zirconia substrate **[22,23]**,~~

~~(vi) the insertion of an active metal in the braze such as Ti (with a content in-between 2 and 5% **[1,2,4]**). The active metal modifies the surface chemistry of the ceramics, diminishes its surface energy by forming an intermediate reaction layer and reduces the contact angle of the melted braze on YSZ **[2,18,21,24]**.~~

~~It is the latter solution, that is the insertion of Ti active metal in the braze, which was chosen during the current study. A satisfactory braze must wet but should also be ductile and bond strongly **[20]**. The Ag-Cu braze is a ductile solvent in which Ti has a very high activity coefficient, which is the relevant thermodynamic parameter that governs the interfacial reaction **[25]**, so that there is no major reservoir of Ti from which too thick brittle reaction product layers may form.~~ With regard to wetting, t~~T~~he contact angles obtained (figures 5 and 6) are lower than 90°, which proves a suitable wettability of YSZ by the active braze and the existence of strong chemical interactions, according to **[~~25~~20]**. During sessile drop method, Ti from the braze was supposed to migrate towards the liquid braze / YSZ interface and to react with oxygen coming from YSZ to form a TiO_2 layer at the interface according to literature data **[~~26~~27]**; the energy of formation of TiO_2 at 900°C is low and amounts to -732 kJ/mol **[~~15~~24]**. The interfacial compounds nature indeed depends on brazing temperature and duration (which promote elements diffusion), on active metal content in braze, on braze thickness **[~~27~~28]** and on the respective nature of the materials of both braze and substrate. Because of the very low surface energy of TiO_2 solid (γ_{sv}=0.8-0.167×10^{-3}×T (J/m²)) **[~~26~~27]**, the Ticusil contact angle decreases and amounts to a value close to 50° for YSZ in the current sessile drop experiment (figures 5 and 6), which is consistent with literature data where a contact angle of 50° under vacuum at 820°C was measured (table of Annex A) **[~~26~~27]**.

The braze contact angle decreases with brazing temperature (figures 5 and 6a) and with holding time at brazing temperature (figure 6b), which is consistent with results reported in

literature [~~25,28~~20,29]. Figure 6 indicates a contact angle of 49° after 30 min at 900°C while a stabilized contact angle of 22° is reached in literature after the same duration at 950°C [~~29~~30]. The distinct results can be explained at least by the difference of brazing temperature and of vacuum quality (table of Annex A). Some authors actually claim the dependence of contact angle with brazing atmosphere [~~27~~28].

Besides, a decrease of the YSZ substrate roughness is shown to reduce the contact angle (figure 6a) at least of 10° for the three tested brazing temperatures. This tendency agrees with data reported in literature [~~30~~31]. A good wetting requires a minimum number of porosities, cracks and asperities on the ceramics surface **[4]**. By the way, it is suggested in literature that ceramic should not present open porosities otherwise they could be filled by the braze which would behave as stresses raiser, harmful for the joint mechanical resistance [~~24~~19]. The dependence of contact angle on substrate roughness is however controversial in literature **[4]** and three theories have been proposed to explain the effect of roughness on contact angle [~~30~~31]:

(i) a thermodynamic approach of Wenzel for which an extra area of surface generated by the substrate roughness leads to an increase of surface energy by assuming that the substrate surface features are low compared to drop dimensions and that their geometry affects only the surface area. This would entail an increase of contact angle for wetting liquids.

(ii) according to Shuttleworth and Bailey, the asperities on rough surfaces could create some barriers which hinder liquid flow attempting to take up the minimum energy contact angle predicted by Wenzel. With this theory, the contact angle would increase with both wetting and unwetting liquids.

(iii) according to Dettré and Johnson, Huh and Mason, Eick and Good, the asperities are some energy barriers which have to be overcome when the liquid front goes ahead and spreads on the surface. With this theory, the contact angle will decrease if the vibrational energy of the liquid (linked to its enthalpy) is greater than the energy barriers to overcome.

Some authors finally assert that, with regard to contact angle, for reactive systems, the relevant roughness to consider in brazing is that of the reaction product which is in direct contact with liquid during braze drop spreading, rather than that of substrate [~~27~~28].

Concerning the substrate surface nature in the case of YSZ ODS Fe based MMC, the presence of chemical heterogeneities inducing also various surface states may also modifiy the contact angles and lead to different local contact angles according to the phase nature on the susbtrate, as suggested in literature [~~25~~20].

Finally and although it has not been investigated in the current study, the contact angle can also depend on crystallographic texture of the substrate and on the polycrystalline or monocystalline feature of the substrate [~~28~~29].

4.1.1.2. Spreading kinetics

Given the typical diffusion coefficient of chemical elements in molten alloy of 5×10^{-9} m²/s, the distance covered by Ti in the liquid braze is at most of 1.8 mm (this height corresponds to the Ticusil™ drop height in figure 5, and figure 4 further shows that Ti layer is intercalated in-between Ag-Cu alloy) which implies that the experimental time required to initiate spreading is lower than 650 s at 900°C. The Ti concentration into the braze however evolves with brazing time.

According to the Reaction Product Control model, the contact angle in a braze-ceramic reactive system with the formation of a new compound at the braze-substrate interface evolves between the initial contact angle θ_0 (defined as the contact angle of the substrate which has not reacted) and the final contact angle θ_f (which is the contact angle on

the reaction product) [~~25~~20]. In the current case, θ_0 amounts to 57.5° and θ_f to 49°, θ_f being linked to the formation of interfacial TiO_2 at 900°C (figures 5 and 6b). In addition, 1200 s are required to obtain a stationary contact angle (figure 6b), which is in agreement with the usual spreading duration limited by the interfacial reaction in braze-ceramic reactive system over the [10-10^4 s] range [~~25~~20]. According to literature [~~35~~32], the logarithmic plots of the ratio $(\cos\theta_f - \cos\theta) / (\cos\theta_f - \cos\theta_0)$ (with θ, instantaneous angle contact angle) *vs*. brazing holding time at 900°C gives a kinetic constant with opposite sign of -0.0052 s^{-1} (figure 15), which is in agreement with literature data for reaction-limited spreading [~~29,35~~30,32].

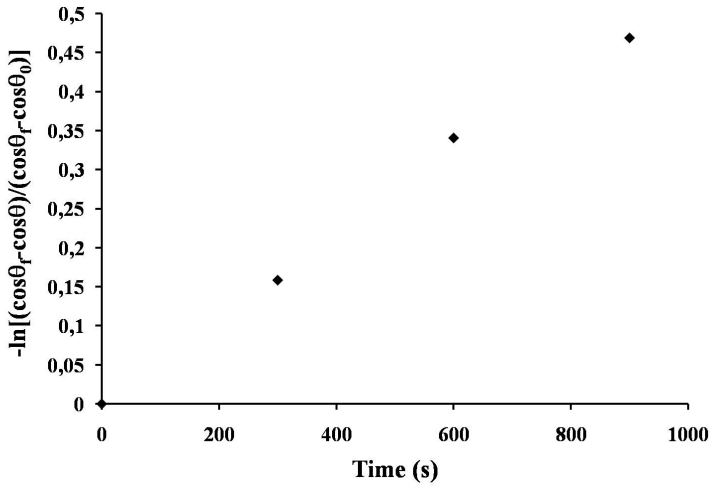

Figure 15: Spreading kinetics of the Ticusil braze drop on YSZ substrate at 900°C (sessile drop method).

4.1.1.3. Work of adhesion

The strength of the chemical interfacial bonding is governed by the existence of crystal orientation relationships and by a low lattice misfit between the compound formed at the interface and the substrate [~~28~~29]. The quality of the adhesion between the materials to join can be estimated by the wettability [~~36~~33] and also evaluated by the work of adhesion [~~36~~33]. The work of adhesion W_{adh} is defined according to Young-Dupré relationship (Equation 1).

$$W_{adh} = \gamma_{LV} \times (1 + \cos\theta) \qquad \text{Equation 1}$$

with θ contact angle and γ_{LV} surface tension of liquid-vapor interfaces.

According to literature, the addition of Ti in the braze improves the work of adhesion W_{adh} between the ceramic and the braze [~~27~~28].

At 900°C for a brazing duration of 20 min, the contact angle amounts to 49° (figure 6b). By assuming an insignificant effect of Ti on liquid alloy surface tension [~~27~~28] and by extrapolating the Ti surface tension of 1650 mJ/m² at its melting point [~~16~~21] to 1.74 J/m² at 900°C [~~27~~28], which is greater than that of eutectic Ag-Cu of 1 J/m² [~~27~~28], the work of adhesion of Ticusil^{TM} – YSZ would amount to 2.88 J/m², which is greater than those calculated at higher temperatures for other dissimilar brazed joints reported in literature **[34]**.

4.1.2. Reactive brazing

4.1.2.1. Brazing mechanism

The brazed joint very likely forms following the sequential stages displayed in figure 16.

Once the solidus temperature of the braze is reached in the MMC-braze-YSZ stacking (figure 16a), the Ag-Cu alloy begins melting at the MMC-YSZ interface. Because of the

presence of a miscibility gap in the Ag-Cu-Ti system at 900°C given the liquidus projection **[~~37~~35]** and the chemical composition of Ticusil^{TM} braze, there is very likely a separation between a liquid enriched in Ti and a liquid depleted in Ti.

Concomitantly, Ti diffuses through the liquid phase towards both YSZ and the MMC and wets the solid surfaces (figure 16b). As already said, the presence of 5 mass.% Ti in the interlayer renders the braze reactive and Ti is well-known as an active metal which improves the wettability of YSZ by Ag-Cu braze **[~~1,2,41~~1,2,4]**. In addition, figure 8b proves that Fe stemming from the MMC diffuses through the braze (it is worth noting that Fe diffusion through the liquid must modify the wettability results obtained with the sessile drop method performed with Ticusil^{TM} braze on YSZ). Subsequent interdiffusion and chemical reactions occur at interfaces.

On MMC side, Ti, after having diffused through the liquid, diffuses at the solid state into the MMC over a distance of 10 µm and reduces FeO contained in the MMC, leading to Fe and to the formation of a continuous layer of titanium oxide TiO_2 (layer 1). Figure 7 actually displayed a 12 µm large FeO depleted zone in the MMC next to the joint interfacial area, which suggests that O^{2-} from FeO was attracted by Ti and carried through this area to combine with Ti. The formation of TiO_2 on MMC side can be explained by the high chemical affinity between Ti and O and by its low energy of formation of -739.5 to -652.7 kJ/mol over [727-1227°C] **[~~15~~24]** (table 2). TiO_2 is further more stable than $Fe_{0.95}O$ whose energy of formation amounts to -197.2 kJ/mol to -165.8 kJ/mol over [727- 1227°C] **[~~15~~24]**, which justifies the FeO reduction by Ti. At a less extent, TiO_2 in layer 1 may also further result from the combination of Ti and O^{2-} stemming from YSZ reinforcements of the MMC.

Concerning the formation of layer 2, figure 8c and d depicts the presence of eutectic constituent between layer 1 and layer 2. Two assumptions may thus be formulated to explain the formation of layer 2 at TiO_2-braze interface:

(i) Layer 2 was formed in the liquid: some Fe, either resulting from FeO reduction or initially contained in the MMC, was dissolved in the liquid phase and reacted with the decomposition products of TiO_2 at high temperature to form, under a low partial pressure of oxygen, $Ti_3Fe_2O_9$ and $TiFeO_3$;

(ii) Layer 2 was formed at solid state by combination of both TiO_2 (layer 1) and Fe (resulting from FeO reduction and present in the MMC) or FeO to form $Ti_3Fe_2O_9$ and $TiFeO_3$.

It is worth noting that both pseudo-rutile $Ti_3Fe_2O_9$ **[~~38,39~~36,37]** and ilmenite $TiFeO_3$ **[~~40~~38]** have already been identified in mineralogy field as $Fe_2O_3.3TiO_2$ and $FeO.TiO_2$ respectively. TiO_2 is also well-known to be able to accept a high amount of FeO (~ 48 mass.%) in solution **[~~41~~39]**. The pressure applied during brazing on this thick brittle layer 2 may also have initiated some cracks leading to the eutectic penetration at layer 1 – layer 2 interface.

Because of the very low solubility of Cu into Ag **[~~15~~24]** and of Fe and Ti diffusion in liquid phase, some oxidized Ti, Fe, Cu bearing particles are formed in the braze (layer 3). During solidification, a eutectic constituent with 91Ag6Cu2Fe*x*O and 87.5Ti8.3Fe4.2Cu*y*O phases is formed at the joint interface (layer 3) (figure 16b).

On YSZ side, some O from YSZ migrates towards the YSZ-braze interface (the long range transport of oxygen ions occurs by hopping between anion sites in YSZ via the vacancies **[~~28~~29]**) and is subsequently very likely dissolved in the braze (Ag presents a very low chemical affinity for O but can dissolve a big amount of O **[~~25~~20]**). It is worth noting that there is no complete reduction of YSZ in Zr by Ti since ZrO_2 is more thermally stable than TiO_2 according to Ellingham diagram **[~~42~~40]**. Since the addition of Y^{3+} cations in ZrO_2 lattice introduces oxygen vacancies **[~~28~~29]**, the O depletion of YSZ during brazing generates a greater density of oxygen vacancies in YSZ lattice. It has already been suggested that Ti can partially deplete zirconia in oxygen **[~~4,29,43,44,4~~,30,41,42]** via the likely formation of a Ti-O complex oxide **[~~43~~41]**; then the freed-up oxygen atoms combine with titanium atoms to form

titanium oxides which present a low Gibbs energy [~~43~~41]. This oxide layer, whose formation is presumably fast, is expected to hinder the dissolution of YSZ in the braze **[18]** contrary to observations reported in literature [~~43~~41]. The layer 4 thus results from the diffusion of Fe stemming from the composite through the liquid phase over a distance of 10 µm towards the braze-YSZ interface and its combination with Ti and O to form $Ti_3Fe_2O_9$ and $TiFeO_3$ according to the mechanisms previously proposed to explain the formation of layer 2.

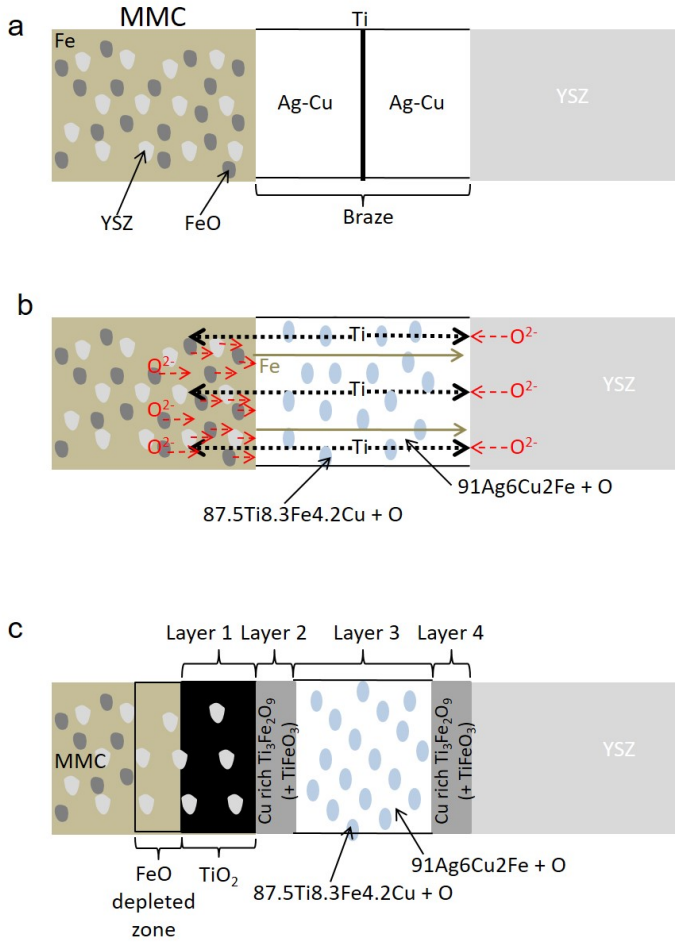

Figure 16: Schematic stages of the formation mechanism of the brazed joint. a) Stacking of MMC, braze and YSZ. b) During heating, diffusion of elements and ions as well as chemical reaction; the arrows indicate diffusion directions. c) At room temperature, architecture of the brazed joint.

Table 2: Energy of formation of compounds (kJ/mol).

Compound	Fe_2Ti	TiO	Ti_2O_3	TiO_2	CuTi	$CuTi_2$	Cu_4Ti	Cu_4Ti_3	Cu_2O	Ti_3Cu_3O
727°C	-	-447.1	-245.7	-739.5					-95.5	
900°C	-67.9	-	-	-	-14.7	-6.6	-3.2	-7.1		-520.5
1227°C	-	-402.7	-116.5	-652.7					-59.5	
Reference	~~45~~43		~~15~~24		**18**		~~46~~44		~~15~~24	**18**

4.1.2.2. *Phases nature*

The $Ti_3Fe_2O_9$ and $TiFeO_3$ phases observed along the brazed joint differ from the phases usually observed in literature during steel or Ti - YSZ brazing with Ag-Cu-Ti interlayer (table of Annex A), namely

- Fe_2Ti [~~32,33~~45,46],
- Ti_xO_y such as Ti_2O_3 [~~32,33~~45,46], TiO, Ti_2O **[18]**,

- Fe_2TiO_4 **[~~32,33~~45,46]**,
- Cu_xTi_y such as $CuTi_3$, Cu_4Ti_3 **[~~18,22,23~~15,16,18]**, CuTi, Cu_4Ti, $CuTi_2$ **[18]**,
- Ti_3Cu_3O **[~~18,22,23~~15,16,18]** which is a M_6X type compound presenting a metallic feature (electrical resistivity of 5×10^{-6} Ω.m) and a very good wettability **[~~27~~28]**,
- Cu_2O **[18]**,
- Ti, Y and Zr bearing phase, Ag, Cu, Ti, Y and Zr bearing phase **[34]**,

and whose available energy of formation of most of them is tabulated in table 2.

The $Ti_3Fe_2O_9$ and $TiFeO_3$ ternary compounds of the braze / YSZ interfacial layer differ from the TiO_2 usually detected during such an experiment with Ticusil^{TM} braze **[~~26~~27]** because of the diffusion of Fe stemming from the MMC through the braze. The energy of formation of $FeTiO_3$ is -26.4 to -24.8 kJ/mol over [727-1227°C] **[~~15~~24]**, but no data about that of $Ti_3Fe_2O_9$ could be found in literature. Since the energy of formation of $FeTiO_3$ is greater than that of TiO_2 (table 2), the kinetics of formation of $Ti_3Fe_2O_9$ and $TiFeO_3$, and the local chemical enrichment can very likely explain the formation of these phases on both sides of the braze.

4.1.2.3. Thickness and morphology of interfacial zones

The Ti bearing global layer (layer 1 + layer 2) at the MMC-braze interface is thicker than layer 4 at braze-YSZ interface, while layer 2 and layer 4 present the same thickness and nature (figures 7 and 8). There was actually a competition between YSZ and MMC to attract Ti. As there was two O available sources on MMC, namely FeO and YSZ, the Ti bearing global layer (layer 1 + layer 2) at the MMC-braze interface is thicker. In addition, YSZ already presents some oxygen vacancies. The formation of layer 4 at the braze – YSZ interface consumes some oxygen from YSZ, which introduces more oxygen vacancies in YSZ and may entail its destabilization.

With regard to the interfacial layers morphology, the braze – YSZ interface is rather straight while the braze – MMC interface is wavy (figures 7 and 8). According to roughness maps in figure 1d and f, the mean roughness parameter of YSZ is slightly smaller than that of MMC. Moreover, the roughness amplitude of the braze – MMC interface which amounts 8 µm (figures 7 and 8a) is greater than the 1.3 µm roughness amplitude of the MMC surface (figure 1f). The existence of a wavy and thick interfacial zone on MMC side suggests its formation partly at the liquid state, the growth of the layers being important at liquid state and slower during solidification **[47]**.

4.2. Diffusion welding

Diffusion welding is recommended in literature to join MMCs provided the thermal cycle is mastered in order to preserve the fineness of the MMCs microstructure **[7]**. In the current study, it is worth noting that the thermal cycle presented in figure 1 enabled the sintering of the graded composite and the concomitant diffusion welding of the ceramic to the graded composites.

The finely polished YSZ and MMC present a Ra of 63 and 74 nm, respectively (figure 2) which is lower than the maximal 0.4 µm surface roughness recommended in literature for diffusion welding **[2,3,7]**. In addition, the melting temperatures of Fe and ZrO_2 are respectively 1538°C and 2690°C while the diffusion welding temperature amounts to 1250°C. The homologous temperatures (HT defined as the ratio between the processing absolute temperature and the absolute melting temperature of the material) for Fe and YSZ are thus respectively 0.84 and 0.51. These values agree well with literature which recommends proceeding either a few hours at a HT of 0.5-0.6 or few minutes at a HT of 0.9 **[2,3,7]**. Young moduli of Fe and ZrO_2 are respectively 221 and 220 GPa **[~~15~~24]** while the coefficient of

thermal expansion (CTE) of YSZ and Fe are respectively 8.9-10.6×10^{-6} °C^{-1} [~~34,43~~34,41] and 12.1×10^{-6} °C^{-1} [~~15~~24]. Since the values of these parameters are rather close for both materials, it suggests once again that these materials were suitable to be joined by diffusion welding [~~28~~29].

The applied low pressure of 50 kPa (compared to that recommended between 1 and 200 MPa **[3]**) enabled to deform the Fe based composite compacted particles (which constitute the MMC) and to suppress the cavities at the MMC particles – bulk YSZ interface. An intimate contact was then generated between the MMC composite compacted particles and the bulk YSZ. An atomic bonding was subsequently established via diffusion and the joint interface was formed via solid state sintering of YSZ-YSZ, YSZ-Fe and YSZ-FeO (figure 17).

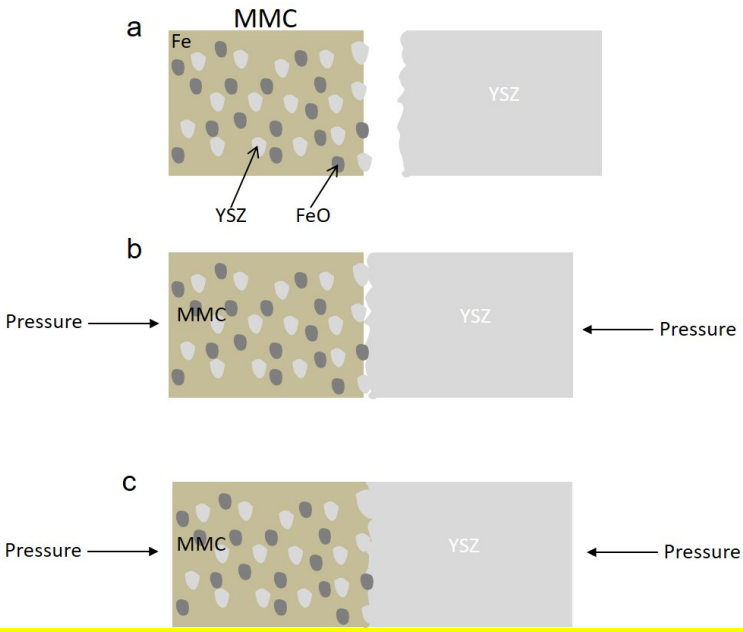

Figure 17: Schematic stages of the formation mechanism of the diffusion joint. a) MMC and YSZ workpieces. b) Beginning of sintering cycle under applied pressure which enables to bring the workpieces into contact. c) During heating, creation of YSZ-YSZ, YSZ-Fe, YSZ-FeO bonds at the joint interface via solid state sintering and formation of the interface.

4.3. Brazing vs. diffusion welding

Concerning the metal-oxide adhesion of MMC and YSZ, two distinct architectural interfaces were developed according to the joining process. As aforementioned, brazing leads to a few micrometers thick oxide layers at the braze-MMC and braze-YSZ interfaces separated by a eutectic phase, while diffusion welding led to discontinuous chemical bonds resulting from YSZ sintering, YSZ stemming from both MMC and bulk YSZ. The mechanical results show that the bending strength and toughness of the diffusion joint is far greater than those of the brazed joint, even if they are rather low (it is worth noting that the test configuration was the most critical since the support was located on the YSZ and its interfaces and did not mimic the real case). The mechanical properties are directly governed by the joints microstructure. It is important to notice that for both joints in the current study, the ceramic YSZ, which presents a small number of slip systems, a low toughness, a low ability to plastic deformation and spontaneous crack propagation **[4]**, is not the most critical defect (figures 11 to 14). Both joints are characterized by a brittle interfacial and non-cohesive

fracture. Concerning the brazed joint, it fractured in the 5 µm (TiO_2) and 1 µm ($Fe_2Ti_3O_9$ and $FeTiO_3$) thick interfacial layers rather than in the ceramic and the eutectic constituent (figures 12, 13). TiO_2 toughness (K_{1c}) amounts to 2.4-3.3 $MPa.m^{0.5}$ **[48]** compared to YSZ toughness (K_{1c}) of 8 $MPa.m^{0.5}$ **[~~15~~24]** while no data were found for $Fe_2Ti_3O_9$ and $FeTiO_3$ compounds. Indeed, according to **[47]**, under shearing solicitations, the brazed joints fracture first through the braze unless (i) the oxides or intermetallic compounds formed at the interfaces occupy a significant fraction of the joint greater than 10% or (ii) the strain rate is high (greater than 0.1 mm/min). Thick and brittle interfacial layers are indeed well-known to be deleterious for the joints mechanical resistance **[~~36~~33]**; a 2 µm thick titanium oxide layer is for instance known to be deleterious for joint mechanical resistance **[~~44~~42]**. With regard to the diffusion joint, fracture occurs at the MMC-YSZ interface (figure 14) but the YSZ-YSZ discontinuous bonds improve the mechanical resistance of the joint, compared to the brazed joint.

Despite the difference of cooling rates during brazing (5°C/min) and diffusion welding (10°C/min) (figure 1), the 3 points bending strength of the diffusion joint is greater than that of the brazed one (figure 10). Even if the temperature during diffusion welding reached 1250°C, joining proceeded at the solid state and the greater cooling rate seems to have not increased as much the residual stresses into the joint. During brazing, the Young moduli mismatches ($E(ZrO_2)$ = 220 GPa **[~~15~~24]**, E(Fe) = 221 GPa **[~~15~~24]**, $E(Ticusil^{TM})$ = 85 GPa **[49]**) and the CTE mismatches (CTE (YSZ) = 9.6×10^{-6} $°C^{-1}$ over [20-400°C] according to the supplier, CTE(Fe) = 14.6×10^{-6} $°C^{-1}$ over [20-800°C] **[~~15~~24]** and $CTE(Ticusil^{TM})$ = 18.5×10^{-6} $°C^{-1}$ **[~~14,34,43~~23,34,41]**) leading to braze shrinkage were expected to generate an elastic mismatch, that is tensile stresses in YSZ and compressive stresses in the braze **[3]**. Indeed, a thermal strain equal to $\Delta\alpha\times\Delta T$, with $\Delta\alpha$: the difference of CTE of YSZ (and Fe) and the braze, and ΔT: the temperature difference between the braze temperature (900°C) and the solidus temperature (which may be, in first approximation, close to Ag-Cu eutectic temperature (figure 8), that is 777°C **[~~15~~24]**), can occur during cooling stage. With the previous data (although they are not rigorous at 900°C), the thermal strains are close to 1.09×10^{-3} at YSZ-braze interface and 4.79×10^{-4} at Fe-braze interface. These values suggest that strain accommodation may occur via interfacial plastic flow due to a suitable ductility of Ag-Cu based braze **[34]**.

Compared to brazing, which is an additional step to the elaboration stage of the MMC, diffusion welding occurs concomitantly with MMC sintering, which is cost-effective even without taking into account the braze price. Diffusion welding further presents the advantage of avoiding an additional coarsening of the MMC microstructure. Besides, the use of a Cu bearing braze to join the MMC and YSZ is not particularly suitable since it (i) can diffuse into Fe favoring its embrittlement and (ii) may entail corrosion, harmful for the aimed application.

4.4. Ways of optimization

Brazing – The applied load on the stacked materials during brazing could be optimized by taking into account the wetting properties and the braze viscosity in order to reduce the interfacial layers thicknesses **[~~36~~33]** which constitute the weak mechanical areas in the current study. Besides, thin reaction zones at the brazed joint interfaces may also be obtained by induction brazing which should require a shorter thermal joining cycle **[4]**.

The enhancement of the mechanical resistance of the braze may be solved (i) by the improvement of the interfaces quality, (ii) by the development of an architectural braze such as a metallic foam (ex: 316L stainless steel) filled by the braze **[8]** or (iii) by the addition of a controlled volume fraction of ceramic particulate reinforcements [**~~3,4,24,50~~3,4,19,50**] in the braze.

According to figure 1a, the 5°C/min cooling rate during the brazing cycle was chosen so as to limit the thermal residual stresses into the joint. Nevertheless and as mentioned with regard to brazing, the mismatch of both Young moduli and CTE between YSZ, the braze and the MMC generate some thermal residual stresses in particular in YSZ where the stresses are the greatest near the joint interface, which can lead to joint fracture in this area. These stresses depend, *inter alia*, on the braze thickness and on the materials size **[4,244,19]**. It was shown that the amplitude of residual stresses increases with the ceramic thickness **[51]**. The 50 µm thickness of the braze used in the current study is usual and the YSZ thickness is already rather low. In order to tempt to tackle the problem of residual stresses, various solutions can be proposed provided they do not diminish the wetting effect of Ti: (i) the addition of a buffer interlayer to the braze **[2]**, this interlayer being ductile (for instance Ag, Cu, Pd, Au, Ni) **[4,324,45]**, (ii) the addition, to the braze, of interlayers with graded CTE **[1,4,8,361,4,8,33]**, (iii) the use of filler metals or alloys, with CTE similar to those of ceramics **[2114]** and (iv) the insertion of a 'braze joint design' which maintains the ceramic in a compressive state **[2114]**.

Diffusion welding – One or several interlayers may be added at the ceramic-MMC interface to assist joining and to adapt the stresses repartition after welding **[3,7]**.
The metal-to-ceramic adhesion bonds may finally be enhanced by performing sintering under microwave fields characterized by a short sintering duration. These adhesion bonds were shown to be increased of about 200-300% compared to those obtained by conventional sintering **[52]**.

5. Conclusions

To summarize, two graded Fe based composite (MMC) – yttria stabilized zirconia (YSZ) joints were developed by brazing, with Ticusil™ braze, and by diffusion welding. The various following points were evidenced:

- Ticusil™ braze presented a better wettability on smooth YSZ substrate. Wetting further increased with brazing temperature.
- The brazed joint was formed by solidification while the diffusion joint was developed by solid state sintering.
- During reactive brazing, some few micrometers thick continuous TiO_2, $Fe_2Ti_3O_9$ and $FeTiO_3$ layers were developed at both the braze-YSZ and braze-MMC interfaces. On the MMC side, TiO_2 was formed by reduction of FeO (contained in the MMC) by Ti. The formation of $Fe_2Ti_3O_9$ and $FeTiO_3$ compounds on the YSZ side resulted from the combination of Fe and Ti which diffused through the braze, and O provided by YSZ and dissolved in the braze.
- During diffusion welding, some YSZ-YSZ, YSZ-FeO and YSZ-Fe discontinuous bonds were created by sintering at the MMC-YSZ interface.
- Both joints fractured at interfaces. The diffusion joint showed the best bending resistance.

Aknowledgments
The authors are very thankful to Ch. Vermander, Ecole Centrale de Lille, France for the brazing TZM device, dies and pistons machining, to P. Denoirjean, SPCTS, Limoges University, France for the wetting analyses, to A.-L. Cristol, LaMcube, Ecole Centrale de Lille, France for her assistance in roughness measurement and to M. Bouhallier, Agence d'Essais Ferroviaires (AEF), France for his help in 3 points static bending tests. They also thank the Microscopy platform of Lille University, France for the use of electron

microscopes. K. Naji is finally grateful to ANRT (French National Association of Research and Technology) for her financial support under CIFRE convention n° 2014/1316.

Annex A

Table: Brazing conditions, interfacial phases and mechanical strength of joints.

Material 1	Material 2	Braze (mass.%) (layer thickness)	Brazing cycle and conditions	Interfacial phases	Strength + fracture location	Reference
YSZ	-	Ag63Cu35.25 Ti1.75	Vacuum (2.5×10^{-6} atm)	TiO_2	-	**~~26~~27**
YSZ (Ra = 0.02 µm)	-	Ag60at-Cu40at-Ti5at (melting T = 788°C)	Vacuum (< 9.8×10^{-11} atm) or pure Ar, Brazing at 950°C, Cooling rate = 4°C/min	4 µm thick layer with Ti and O with various Ti/Cu/O atomic ratios: 54/0/46, 40/30/30 and 3-5µm thick layer of Ti54-Cu27-O19 (at%)	-	**~~29~~30**
ZrO_2	-	Ag-Cu-Ti		Ti_xO at interface and formation of an out-of stoichiometric zirconia	Bending strength of 300 MPa	**3**
YSZ	Ferritic stainless steel	Ag58-Cu32-Pd10 or Ag65-Cu20-Pd15		Cu rich phase containing Zr in solid solution as well as Fe and Cr, Cu_3Pd layer at steel side with 58Ag-32Cu-10Pd and 65Ag-20Cu-15Pd particles and Fe(Cr) needle-like phase, SiO_2 and Ti_3O_5 at YSZ side		**~~31~~53**
YSZ	Ferritic stainless steel (17-19%Cr)	Ag68.8-Cu26.7-Ti4.5 (0.1-0.12 mm) (T liquidus = 900°C)	Vacuum (1.3×10^{-9} atm), Heating up to 915°C, holding time of 5 min at this temperature, Slow cooling up to room temperature, Pressure = 0.3N	Fe_2Ti at steel-braze interface and Ti_2O_3 and Fe_2TiO_4 at braze – YSZ interface.	Tensile strength of 16.7 MPa Shear strength of 40.2 MPa Fracture in braze	**~~32,33~~45,46**
YSZ coated with TiH_2	Stainless steel coated with Ni	Ag72-Cu28 + 25 µm and 2.7 µm sized TiH_2 particles	No pressure	From YSZ to stainless steel: $CuTi_3$, Ti_3Cu_3O, Cu_4Ti_3, $NiTi_2$, Ni_3Ti, Ti	Shear strength of 90 MPa	**~~22,23~~15,16**
YSZ	Ti	Ticusil™ (68.8Ag-26.7Cu-4.5Ti) (0.05 mm)	Vacuum (9.8×10^{-10} atm) and Ar purge, Heating at 5°C/min up to 900°C, holding time	at Ticusil-braze interface: 0.1 h brazing: TiCu and TiO 1 and 6 h brazing: Ti_3Cu_3O, Ti_2O, TiO	-	**18**

			at 900°C of 0.1, 1 et 6 h and 3°C/min cooling rate, Applied pressure = 0.1 MPa,	Along the braze: Ag + $TiCu_4$ for 0.1h, Ag + Cu_2O for 1h and Ag+Cu_2O+(Ag+Ti_3Cu_3 O) for 6h at Ti-braze interface: Ti_2Cu, TiCu, Ti_3Cu_4, $TiCu_4$, α-Ti+Ti_2Cu		
YSZ	Steel	Ticusil™	Brazing at 910°C for 5 min	Ti diffusion in steel; Fe, Cr, Zr and Y diffusion in braze; Ag diffusion in YSZ. Ag and Zr bearing layer at YSZ- Ticusil™ interface; Ti enrichment at YSZ surface; adjacent Ti, Cu, Ag, Zr, Y bearing diffuse layer; Ag-Cu eutectic in braze; Fe, Cr, Ti bearing phases in eutectic constituent on steel side; Zr,Y, Ti bearing phases in eutectic constituent on YSZ side.	-	**34**

References

[1] Suganuma K, Joining ceramics and metals, Handbook of advanced ceramics, Elsevier, Chapter 10.1. 2013; 775-788

[2] Zhang Y, Feng D, He ZH, Chen XC. Progress in joining ceramics to metals. J Iron Steel Res Intern 2006;13(2):01-05

[3] Fernie JA, Drew RAL, Knowles KM. Joining of engineering ceramics. Intern Mater Rev 2009;54(5):283-331

[4] Hausner S, Wielage B. Brazing of metal and ceramic joints, Chap 12, Advances in brazing, Technology and Engineering, Elsevier 2013;361-393

[5] Avettand-Fènoël MN, Nagaoka T, Fujii H, Taillard R. Characterization of WC/12Co cermet – steel dissimilar friction stir welds. J Manuf Proc 2018;31:139-155

[6] Avettand-Fènoël MN, Nagaoka T, Fujii H, Taillard R. Effect of a Ni interlayer on microstructure and mechanical properties of WC-12Co cermet / SC45 steel friction stir welds. J Manuf Proc 2019;40:1-15

[7] Cam G, Kocak M. Progress in joining of advanced materials. Inter Mater Rev 1998; 43(1):1-44

[8] Shirzadi AA, Zhu Y, Bhadeshia HKDH. Joining ceramics to metals using metallic foams. Mater Sci Engin A 2008;496:501-506

[9] Ji GC, Wang HT, Chen X, Bai XB, Dong ZX, Yang FG. Characterization of cold-sprayed multimodal WC-12Co coating. Surf Coat Technol 2013;235:536-543.

[10] Dosta S, Couto M, Guilemany JM. Cold spray deposition of a WC-25Co cermet onto Al7075-T6 and carbon steel substrates. Acta Mater 2013;61:643-652.

[11] Naji K, Avettand-Fènoël MN, Laurans E, Taillard R, Insulating rail gasket,
FR 3045078 B1 delivered on 2017, 29th December
EP 3178991 B1 delivered on 2018, 17th October

[12] Naji K, Marinova M, Touzin M, Pouligny Ph, Avettand-Fènoël MN. Design and characterization of an oxides hybrid dispersion strengthened iron based composite with a graded and architectural microstructure. J All Compounds 2019;802:217-228

[~~20~~13] Nicholas MG, Peteves SD. Reactive joining; chemical effects on the formation and properties of brazed and diffusion bonded interfaces. Scripta Metall Materialia 1994;31(8): 1091-1096

[~~21~~14] Walker CA. Metal-nonmetal brazing for electrical, packaging and structural applications, Chap 16, Advances in brazing: science, technology and applications 2013;498-523

[~~22~~15] Liu GW, Qiao GJ, Wang HJ, Yang JF, Lu TJ. Pressureless brazing of zirconia to stainless steel with Ag-Cu filler metal and TiH_2 powder. J European Ceramic Society 2008;28:2701-2708

[~~23~~16] Liu GW, Li W, Qiao GJ, Wang HJ, Yang JF, Lu TJ. Microstructures and interfacial behavior of zirconia/stainless steel joint prepared by pressureless active brazing. J Alloys Compnds 2009;470:163-167

[17] Bian H, Zhou Y, Song X, Hu S, Shi B, Kang J, Feng J. Reactive wetting and interfacial characterization of ZrO_2 by SnAgCu-Ti alloy. Ceramics Intern 2019;45:6730-6737

[18] Wei SH, Lin CC. Microstructural evolution and bonding mechanisms of the brazed Ti/ZrO2 joint using an Ag68.8Cu26.7Ti4.5 interlayer at 900°C. J Mater Res 2014;29(5): 664-694

[~~24~~19] Blugan G, Kuebler J, Bissig V, Janczak-Rusch J. Brazing of silicon nitride ceramic composite to steel using SiC-particle reinforced active brazing alloy. Ceramics Intern 2007;33:1033-1039

[~~25~~20] Eustathopoulos N. Wetting by liquid metals – application in materials processing: the contribution of the Grenoble Group, Metals 2015;25:350-370

[~~16~~21] Lucas LD, Tension superficielle, Techniques de l'ingénieur, ref M67 V1, 1984

[~~13~~22] Cadden CH. Brazing, Encyclopedia of Materials: Science and Technology, Elsevier 2006;1-7

[~~14~~23] Jacobson DM, Humpston G, Principes of Brazing, ASM International 2005.

[~~15~~24] Smithells Metals Reference Book, 7th edition, Eds: E.A. Bra,des, G.B. Brook, Butterworth Heinemann, Oxford, 1992

[~~17~~25] NF EN ISO 14125, Détermination des propriétés de flexion des composites, 1998

[~~19~~26] Macel D. Avez-vous pensé au brasage?, Soudage et techniques connexes 2016 ;39-45

[~~26~~27] Triantafyllou G, Irvine JTS. Wetting and interactions of Ag-Cu-Ti and Ag-Cu-Ni alloys with cermaic and steel substrates for use as sealing materials in a DCFC stack. J. Mater. Sci. 2016;51:1766-1778

[~~27~~28] Voytovych R, Robaut F, Eustathopoulos N. The relation betxeen wetting and interfacial chemistry in the CuAgTi/alumina system. Acta Mater 2006;54:2205-2214

[~~28~~29] Munoz MC, Gallego S, Beltran JI, Cerda J. Adhesion at metal-ZrO_2 interfaces. Surf sci report 2006;61(7):303-344

[~~29~~30] Muolo ML, Ferrera E, Morbelli L, Passerone A. Wetting, spreading and joining in the alumina-zirconia-Inconel 738 system. Scripta Mater 2004;50:325-330

[~~30~~31] Hitchcock SJ, Carroll NT, Nicholas MG. Some effects of substrate roughness on wettability. J Mater Sci 1981;16:714-732

[~~35~~32] Dezellus O, Hodaj F, Eustathopoulos N. Chemical reaction-limited spreading : the triple line velocity versus contact angle relation. Acta Mater 2002;50:4741-4753

[~~36~~33] Suganuma K. Recent advances in joining technology of ceramics to metals. ISIJ Intern 1990;30(12):1046-1058

[~~34~~34] Singh M, Shpargel TP, Asthana R. Brazing of yttria-stabilized zirconia (YSZ) to stainless steel using Cu, Ag and Ti-based brazes. J Mater Sci 2008;43:23-32

[~~37~~35] Kubaschewski O. Silver-copper-titanium, MSIT, Landolt-Börnstein, New series IV/11B. 144-455

[~~38~~36] Teufer G, Temple AK. Pseudorutile – a new mineral intermediate between Ilmenite and Rutile in the N alteration of Ilmenite. Nature 1966;211:179-181

[~~39~~37] Grey IE, Reid AF. The structure of pseudorutile and its role in the natural alteration of ilmenite. American Mineralogist 1975;60:898-906

[~~40~~38] Harrison RJ, Redfern SAT, Smith RI. In-situ study of the R-3 to R-3c phase transition in the ilmenite-hematite solid solution using time-of-flight neutron powder diffraction. American Mineralogist 2000;85(1):194-205

[~~41~~39] Xuan C, Karasev A, Shibata H, Jönsson PG. Wetting behavior of single crystal TiO2 by liquid iron. ISIJ International 2016;56(5):765-769

[~~42~~40] Philibert J, Vignes A, Bréchet Y, Combrade P. Métallurgie : du minerai au matériau, Masson, Paris, 1998

[~~43~~41] Singh M, Shpargel TP, Asthana R. Brazing of stainless steel to YSZ using silver base brazes, in Advances in ceramic coatings and ceramic metal systems, Zhu D, Plucknett K, Eds., The American Ceramic society, Westerville USA 2005

[~~44~~42] Hanson WB, Ironside KI, Ferne JA. Active metal brazing of zirconia. Acta Mater 2000;48:4673-4676

[~~45~~43] Mao X. Titanium microalloyed steel: Fundamentals, technology and products. Metallurgical Industry Press, Springer, Beijing 2019

[~~46~~44] Liang YH, Wang HY, Yang YF, Wang YY, Jiang QC. Evolution process of the synthesis of TiC in the Cu-Ti-C system,. J Alloys Compnds 452 (2008) 298-303

[~~32~~45] Lin KL, Singh M, Asthana R, Lin CH. Interfacial and mechanical characterization of yttria-stabilized zirconia (YSZ) to stainless steel joints fabricated using Ag-Cu-Ti interlayers. Ceramics Intern 2014;40:2063-2071

[~~33~~46] Lin KL, Singh M, Asthana R. Effect of short-term aging on interfacial and mechanical properties of yttria stabilized zirconia (YSZ)/stainless steel joints. J European Ceramic Soc 2015;35:1041-1053

[47] Frear DR, Vianco PT. Intermetallic growth and mechanical behavior of low and high melting temperature solder alloys. Metall Mater Trans A 1994;25:1509-1523

[48] https://www.azom.com/properties.aspx?ArticleID=1179

[49] Ashtana R, Singh M. Joining of partially sintered alumina to alumina, titanium, Hastealloy and C-Sic composite using Ag-Cu brazes. J European Ceramic Soc 2008;28:617-631

[50] Lin KL, Singh M, Asthana R. Characterization of yttria-stabilized-zirconia / stainless steel joint interfaces with gold-based interlayers for solid oxide fuel cell applications. J European Ceramic Soc 2014;34:355-372

[51] Suganuma K, Okamoto T, Koizumi M, Shimada M. Effect of Thickness on Direct Bonding of Silicon Nitride to Steel. J. Am. Ceram. Soc. 1985;68(12):C-334-C-335

[52] Pan EG, Ravaev AA. The Enhancement of Metal-to-Ceramics Adhesion Bond Under Sintering in Microwave Fields. Adv Engin Mater 2004;6(1-2):61-64

[~~31~~53] Lin KL, Singh M, Asthana R. Interfacial characterization of YSZ-to-steel joints with Ag-Cu-Pd interlayers for solid oxide fuel cell applications. Ceramics intern 2012;38:1991-1998